Comparisons of (±)-Benzo[*a*]pyrene-*trans*-7,8-Dihydrodiol Activation by Human Cytochrome P450 and Aldo−Keto Reductase Enzymes: Effect of Redox State and Expression Levels

Amy M. Quinn[†] and Trevor M. Penning*

Center of Excellence in Environmental Toxicology, Department of Pharmacology, University of Pennsylvania School of Medicine, Philadelphia, Pennsylvania 19104-6084

Received September 21, 2007

Polycyclic aromatic hydrocarbons (PAHs) are environmental pollutants that are metabolically activated to proximate carcinogenic *trans*-dihydrodiols. PAH *trans*-dihydrodiols are further activated in humans by cytochrome P450 (P450) 1A1 and 1B1 to yield diol-epoxides or by aldo−keto reductases (AKR) 1A1 and 1C1–1C4 to yield reactive and redox-active *o*-quinones. Reconstituted *in vitro* systems were used to compare the steady-state kinetic constants for human P450 (P450 1A1 and 1B1) and AKR (AKR1A1, AKR1C1–1C4) mediated metabolism of (±)-*trans*-7,8-dihydroxy-7,8-dihydrobenzo[*a*]pyrene ((±)-B[*a*]P-7,8-diol) at physiological pH. It was found that P450 isoforms yielded much greater k_{cat}/K_m values than AKR enzymes. Initial rates of (±)-B[*a*]P-7,8-diol oxidation were measured for AKR1A1, AKR1C2, P450 1A1, and P450 1B1 as the ratio of NADPH/NAD^+ cofactors was varied to determine the redox state necessary for AKRs to successfully compete for *trans*-dihydrodiols. P450 and AKR enzymes equally competed for (±)-B[*a*]P-7,8-diol substrate at an NADPH/NAD^+ ratio equal to 0.001. The resting NADPH/NAD^+ ratio was determined in A549 human lung adenocarcinoma cells to be 0.28. These data suggest that the P450 pathway would be favored over the AKR pathway if the enzymes were equally expressed. Basal mRNA transcript levels of AKR1C1–1C3 exceed those of both basal and 2,3,7,8-tetrachlorodibenzo-*p*-dioxin (TCDD)-induced P450 1A1 and 1B1 by up to 90-fold in A549 cells as measured by real-time reverse transcriptase polymerase chain reaction (RT-PCR) methods. AKR expression levels were comparable to TCDD-induced P450 1A1 and 1B1 in HBEC-KT immortalized normal human bronchial epithelial cells. Functional assays of both A549 and HBEC-KT cell lysates demonstrated a lack of TCDD-inducible P450 1A1/1B1 activity but robust basal expression of AKR1A1 and AKR1C activities, where the functional assay for P450 detection is 300-fold more sensitive than the functional assay for AKR isoforms. These data suggest that AKR enzymes may effectively compete with P450 1A1/1B1 for PAH *trans*-dihydrodiol activation in human lung cells.

Introduction

Tobacco smoke contains a complex mixture of polycyclic aromatic hydrocarbons (PAHs).[1] B[*a*]P is the most studied PAH and causes lung, skin, and stomach tumors in animals (*1*). Recently, the International Agency for Research on Cancer (IARC) reclassified B[*a*]P as a human carcinogen (*2*). B[*a*]P requires metabolic activation to exert its deleterious effects. There are three proposed pathways of B[*a*]P activation that are applicable to other PAHs. The first involves formation of a radical cation through P450 peroxidase-mediated one-electron oxidation, which results in the formation of depurinating DNA adducts (*3*).

The other two pathways of PAH activation require the consecutive actions of P450 1A1 or 1B1 and epoxide hydrolase to yield proximate carcinogenic *trans*-dihydrodiols, for example, (±)-*trans*-7,8-dihydroxy-7,8-dihydrobenzo[*a*]pyrene (B[*a*]P-7,8-diol), Scheme 1. Further epoxidation of (±)-B[*a*]P-7,8-diol by P450 1A1 and 1B1 using NADPH as a cofactor generates (±)-*trans*-7,8-dihydroxy-9α,10α-epoxy-7,8,9,10-tetrahydrobenzo[*a*]pyrene ((±)-*anti*-BPDE) which has been shown to react with dGuo to form (+)-*trans*-*anti*-BPDE−N^2-dGuo adducts (*4–9*). Error-prone lesion bypass of these adducts leads to mutation of the tumor suppressor *p53* and proto-oncogene *K-ras*, the two genes most frequently mutated in smoking-associated lung cancer (*10, 11*). Both P450 1A1 and 1B1 are expressed in extra-hepatic tissues, including the lung, and are inducible via the aryl hydrocarbon receptor (AhR) agonist 2,3,7,8-tetrachlorodibenzo-*p*-dioxin (TCDD), as well as by PAHs themselves (*12–14*). Additionally, P450 1A1 and 1B1 are up-regulated in lung tissue of smokers (*15, 16*).

* To whom correspondence should be addressed. Mailing address: Department of Pharmacology, University of Pennsylvania, School of Medicine, 130C John Morgan Bldg., 3620 Hamilton Walk, Philadelphia, PA 19104-6084. Phone: (215) 898-9445. Fax: (215) 573-2236. E-mail: penning@pharm.med.upenn.edu.

[†] E-mail: aquinn@mail.med.upenn.edu.

[1] Abbreviations: ACN, acetonitrile; AhR, aryl hydrocarbon receptor; AKR, aldo−keto reductase; ANOVA, analysis of variance; ARE, antioxidant response element; BICINE, *N*,*N*-bis(2-hydroxyethyl) glycine; B[*a*]P, benzo[*a*]pyrene; (±)-B[*a*]P-7,8-diol, (±)-*trans*-7,8-dihydroxy-7,8-dihydrobenzo[*a*]pyrene; (±)-*anti*-BPDE, (±)-*trans*-7,8-dihydroxy-7,8-dihydro-9α-epoxy-7,8,9,10-tetrahydrobenzo[*a*]pyrene; BSA, bovine serum albumin; DE1, (±)-B[*a*]P-*r*-7,*t*-8-dihydrodiol-*c*-9,10-epoxide; DE2, (±)-B[*a*]P-*r*-7,*t*-8-dihydrodiol-*t*-9,10-epoxide; EROD, ethoxyresorufin O^7-deethylation; GAPDH, glyceraldehyde-3-phosphate dehydrogenase; G6P, glucose-6-phosphate; G6PD, glucose-6-phosphate dehydrogenase; 8-oxo-dGuo, 8-oxo-2′-deoxyguanosine; MOPS, 3-(*N*-morpholino)propanesulfonic acid; MTT, 3-(4,5-dimethylthiazol-2-yl)-2,5-diphenyltetrazolium bromide; P450, cytochrome P450; PAHs, polycyclic aromatic hydrocarbons; PBGD, porphobilinogen deaminase; PES, phenazine ethosulfate; ROS, reactive oxygen species; RT-PCR, reverse transcriptase polymerase chain reaction; TCDD, 2,3,7,8-tetrachlorodibenzo-*p*-dioxin; (±)-B[*a*]P-tetraol 1, *r*-7,*t*-8,*t*-9,*c*-10-(±)-B[*a*]P-tetrahydrotetraol.

10.1021/tx700345v CCC: $40.75
Published on Web 04/11/2008

Scheme 1. Pathways of PAH *trans*-Dihydrodiol Activation

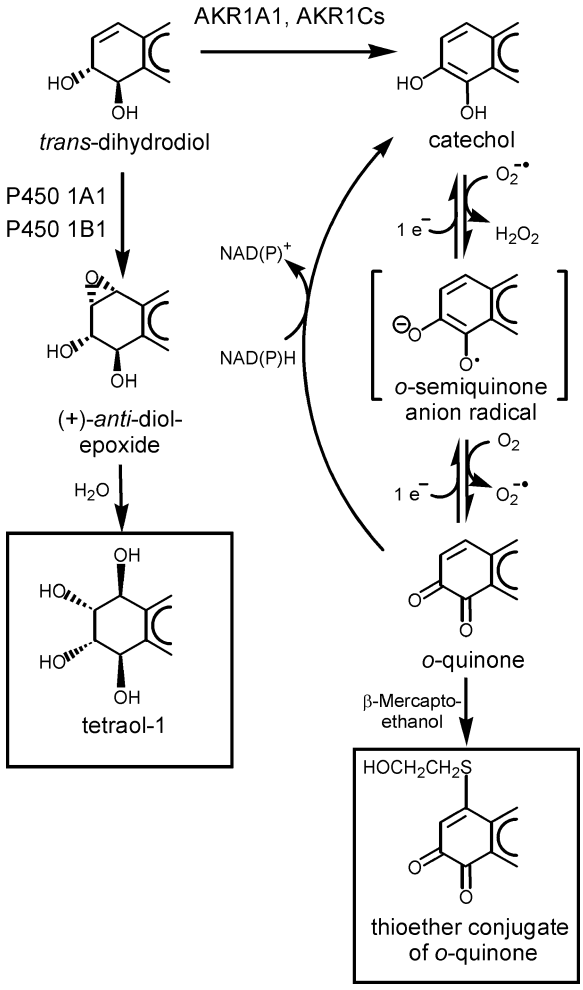

Alternatively, members of the AKR superfamily, including human aldehyde reductase AKR1A1 and the human hydroxysteroid dehydrogenases AKR1C1−AKR1C4, will oxidize the P450-generated PAH *trans*-dihydrodiols in an $NAD(P)^+$-dependent manner to produce *o*-quinones such as B[*a*]P-7,8-dione (*17, 18*). PAH *o*-quinones are electrophilic species that can form stable and depurinating adducts with DNA (*19–22*). PAH *o*-quinones are also redox-active molecules that can undergo redox-cycling to produce reactive oxygen species (ROS). This amplification of ROS may lead to a change in cellular redox state and the formation of oxidatively damaged bases, for example, 8-oxo-2′-deoxyguanosine (8-oxo-dGuo) (*23–27*). Under redox-cycling conditions, B[*a*]P-7,8-dione is a potent mutagen of *p53 in vitro*, resulting primarily in guanine to thymine (G → T) transversions, which dominate mutations in lung tumors (*28, 29*).

AKR1A1 and AKR1C1−AKR1C3 are widely expressed in human tissues; however, AKR1C4 is liver-specific. AKR1C transcripts are overexpressed in non-small-cell lung carcinoma and are positively correlated with poor prognosis (*30*). Up-regulation of AKR1C1 and AKR1C2 has also been observed in non-small-cell lung carcinoma and squamous cell carcinoma of the esophagus (*31–33*).

It is thus important to compare the relative contributions of the P450 and AKR pathways in the metabolic activation of PAH *trans*-dihydrodiols. Here we compare the *in vitro* kinetic parameters for (±)-B[*a*]P-7,8-diol monooxygenation and oxidation at physiological pH. The effect of redox state on determining which pathway is favored was examined by varying cofactor ratios. We show that the P450 pathway dominates kinetically in (±)-B[*a*]P-7,8-diol activation on a mole-for-mole basis. However, when the redox state is manipulated, the AKRs can play a more prominent role. Nicotinamide adenine dinucleotide cofactors [NAD(H) and NADP(H)] were measured in A549 cells and found to be available for both P450- and AKR-mediated metabolism of PAH *trans*-dihydrodiols. The A549 human lung adenocarcinoma cell line is a well-established and characterized model of type II alveolar epithelial cells and has been used extensively to study TCDD regulation of P450 enzymes (*34–36*). As a transformed cell line, A549 cells may not accurately depict the tissue microenvironment of normal human lung. Nonmalignant human bronchial epithelial HBEC-KT cells, immortalized by ectopic expression of hTERT and inactivation of the p16/pRb pathway, were used to represent "normal" lung epithelium (*37*). When the expression levels of AKR enzymes are considered along with their ability to alter redox state, it is likely that this will offset kinetic differences to allow effective competition of AKRs for PAH *trans*-dihydrodiol substrates in lung cells.

Experimental Procedures

Caution: *All PAHs are potentially dangerous and were handled in accordance with NIH Guidelines for the Use of Chemical Carcinogens.*

Chemicals. The following chemicals were purchased from Sigma-Aldrich (St. Louis, MO): ethoxyresorufin, resorufin, glucose-6-phosphate (G6P), glucose-6-phosphate dehydrogenase (G6PD, *Saccaromyces cerevisiae*), thiazolyl blue tetrazolium bromide (MTT), and phenazine ethosulfate (PES). [^{3}H]-(±)-B[*a*]P-7,8-diol, (±)-B[*a*]P-7,8-diol, *r*-7,*t*-8,*t*-9,*c*-10-benzo[*a*]pyrene-tetrahydrotetraol ((±)-B[*a*]P-tetraol 1), and TCDD were obtained from the NCI Chemical Carcinogen Standard Reference Repository (Midwest Research Institute, Kansas City, MO). 1-Acenaphthenol and *p*-nitrobenzaldehyde were purchased from Fisher Scientific Intl. (Pittsburgh, PA). Flufenamic acid was obtained from ICN Biomedical Inc. (Aurora, OH). Ponalrestat was provided courtesy of Dr. Florante Quiocho (Baylor College of Medicine, Houston, TX).

Enzymes. All AKRs were expressed as recombinant enzymes and purified to homogeneity according to published procedures (*17, 38*) to yield enzymes of the following specific activities: 6.0 μmol of *p*-nitrobenzaldehyde (1 mM) reduced/(min mg) (AKR1A1); 0.21 μmol of androsterone (75 μM) oxidized/(min mg) (AKR1C4); and 2.1, 2.5, and 2.8 μmol of 1-acenaphthenol (200 μM) oxidized/(min mg) (AKR1C1, AKR1C2, and AKR1C3, respectively). P450 1A1 and 1B1 Supersomes were purchased as baculovirus-infected insect cell microsome preparations from BD Gentest (Woburn, MA). Amounts of P450 used in kinetic assays were determined by comparison of measured rates of ethoxyresorufin O^7-deethylation (EROD) activity with those reported in product inserts. Specific activities for P450 1A1 and P450 1B1 were 2.6 and 1.2 nmol of ethoxyresorufin O^7-deethylated/(min mg), respectively.

Determination of Steady-State Kinetic Parameters. To determine the kinetic constants for the monooxygenation of (±)-B[*a*]P-7,8-diol catalyzed by P450 isoforms, incubations contained 0.25–20 μM [^{3}H]-B[*a*]P-7,8-diol (5×10^5 cpm/nmol) in 8% DMSO and an NADPH-regenerating system (1.3 mM $NADP^+$, 3.3 mM G6P, 0.4 U/mL G6PD, 3.3 mM magnesium chloride) in 50 mM MOPS buffer, pH 7.4, containing 400 μM β-mercaptoethanol and P450 Supersomes (P450 1A1 0.3 pmol, P450 1B1 2.5 pmol) in a final volume of 500 μL. End-point reactions were performed in duplicate over 60 min at 37 °C. Initial rates of both (±)-B[*a*]P-7,8-diol consumption and formation of (±)-B[*a*]P-tetraol 1 were monitored, and steady-state kinetic parameters (k_{cat}, K_m, and k_{cat}/K_m) were determined for (±)-B[*a*]P-7,8-diol oxidation. Rapid hydrolysis of P450-generated diol epoxides occurs nonenzymatically to generate (±)-B[*a*]P-tetraols. Formation of the more carcinogenic *anti*-diol epoxide (±)-B[*a*]P-*r*-7,*t*-8-dihydrodiol-*t*-9,10-epoxide (DE2) from

racemic (±)-B[*a*]P-7,8-diol is favored over the *syn*-isomer (±)-B[*a*]P-*r*-7,*t*-8-dihydrodiol-*c*-9,10-epoxide (DE1) for P450 1A1 and 1B1. Hydrolysis of each diol epoxide produces a pair of tetraols, with DE2 hydrolysis proceeding *trans* stereoselectively at the C10 position, yielding the major product (±)-B[*a*]P-tetraol 1 (*39*).

To determine the steady-state kinetic parameters for (±)-B[*a*]P-7,8-diol oxidation catalyzed by the human AKR isoforms, incubations contained 1.25–80 μM [^{3}H]-B[*a*]P-7,8-diol (5×10^5 cpm/nmol) with a final concentration of 8% DMSO and 2.3 mM $NADP^+$ in 50 mM MOPS buffer, pH 7.4, containing 400 μM β-mercaptoethanol and AKR enzyme (AKR1A1 2.0 μg, AKR1C1 5.0 μg, AKR1C2 1.25 μg, AKR1C3 4.0 μg, AKR1C4 2.0 μg) in a final volume of 500 μL. End-point reactions were performed in duplicate over 60 min at 37 °C. Following the observation that trapping of B[*a*]P-7,8-dione is stoichiometric (*40*), initial rates of B[*a*]P-7,8-dione thioether conjugate production were monitored in addition to rates of (±)-B[*a*]P-7,8-diol consumption.

P450 and AKR reactions were terminated by addition of 500 μL of ice-cold acetone and extracted twice with 1 mL of ethyl acetate. B[*a*]P-4,5-diol (0.5 nmol) was used as an internal standard to correct for extraction efficiency. Combined extracts were dried under vacuum and redissolved in methanol for analysis by reversed-phase HPLC. Reaction products were separated using a Waters Alliance 2695 HPLC system (Waters Corp., Milford, MA) with a Zorbax-ODS C18 column (5 μm, 4.6 mm × 250 mm; Agilent Technologies, Palo Alto, CA) and a flow rate of 0.5 mL/min. Separation of P450 reaction products was done with 50% methanol (v/v) for 10 min, followed by a linear gradient of 50–90% methanol (v/v) for 60 min. AKR reaction products were separated with a linear gradient of 70–76% methanol (v/v) over 40 min. Elution was monitored with a Waters 2996 photodiode array detector and β-RAM in-line radioactive detector (IN/US Systems Inc., Tampa, FL). Product identity was verified by comparison of retention times and UV spectra with those of authentic standards. Calculation of initial rates (nmol/min) was achieved both by comparison of peak areas to standard curves constructed for each compound at the wavelength of maximum absorption (272.2 nm for B[*a*]P-4,5-diol, 364.7 nm for (±)-B[*a*]P-7,8-diol, 343.3 nm for (±)-B[*a*]P-tetraols, and 254 nm for the thioether conjugate of B[*a*]P-7,8-dione) and by comparison of peak areas to a standard curve constructed for [^{3}H]-B[*a*]P-7,8-diol using the β-RAM detector in the tritium channel. Data were normalized to the B[*a*]P-4,5-diol internal standard and analyzed by fitting velocity versus substrate concentration data to the equation for a hyperbola, $v = V_{max}[S]/(K_m + [S])$ to generate the mean ± standard error for steady-state kinetic parameters. Values were corrected for inhibition by 8% DMSO (AKR1A1 27.7%, AKR1C1 44.8%, AKR1C2–1C4 100%, P450 1A1 87.7%, P450 1B1 36.9% remaining activity).

Effect of Cofactor Ratios on Preferred Oxidation Pathway. Specific activities for the consumption of 10 μM (±)-B[*a*]P-7,8-diol were measured using AKR1A1, AKR1C2, P450 1A1, or P450 1B1 as the cofactor ratio was varied. Incubations were performed in 250 μL of 50 mM MOPS buffer, pH 7.4, containing 8% DMSO. All reactions contained 1 mM NAD^+ and NADPH was varied from 0.001 to 1.0 mM in final concentration. End-point assay reactions were performed in duplicate over 60 min at 37 °C.

Cell Culture. Human lung adenocarcinoma A549 cells were obtained as a kind gift from Dr. S. Aaronson (Mount Sinai School of Medicine, New York, NY). Cells (5×10^6) were maintained in 100-mm dishes at 37 °C and 5% CO_2 containing 10 mL of DMEM media supplemented with 10% fetal bovine serum, 2 mM L-glutamine, 100 U/mL penicillin, and 100 μg/mL streptomycin. Cells were treated for 12 h with either 0.1% DMSO or 10 nM TCDD to induce P450 expression.

HBEC-KT cells were a kind gift from Dr. J. D. Minna (University of Texas Southwestern Medical Center, Dallas, TX). Cells were maintained in 100-mm plates coated with porcine skin gelatin, type A (Sigma-Aldrich, St. Louis, MO), in keratinocyte serum-free media with supplements (Invitrogen, Carlsbad, CA). Cells were treated for 12 h with either 0.1% DMSO or 10 nM TCDD to induce P450 expression.

Nicotinamide Adenine Dinucleotide Cofactor Measurement. NADH and NADPH were extracted from A549 cells with alkaline treatment to destroy oxidized cofactor. Cells were scraped into 1 mL of 0.5 M NaOH per 100 mm dish and incubated at 60 °C for 10 min. Solutions were neutralized with 0.25 mL of ice-cold 1 M H_3PO_4 and cooled on ice. NAD^+ and $NADP^+$ were extracted from A549 cells with acid treatment to destroy reduced cofactor. One milliliter of 0.5 M $HClO_4$ was added to each 100 mm dish, and cells were incubated on ice for 15 min. Cells were scraped and neutralized with 0.5 mL of 1 M KOH. Acid- and base-treated neutralized solutions were centrifuged at 1500 rpm for 10 min at 4 °C to remove cell debris and insoluble $KClO_4$. An aliquot of supernatant was removed for analysis of protein concentration. Supernatants were filtered using a 10 kDa membrane (Millipore) at 1500 rpm for 15 min at 4 °C.

Concentrations of NAD^+ and NADH were determined by the modified enzymatic cycling assay of Jacobson and Jacobson (*41*). Briefly, pyridine nucleotide extracts were preincubated with 500 mM ethanol, 0.42 mM 3-(4,5-dimethylthiazol-2-yl)-2,5-diphenyltetrazolium bromide (MTT), 1.66 mM phenazine ethosulfate (PES), and 4.16 mM EDTA in 100 mM Na-Bicine buffer, pH 8.0, for 5 min at 37 °C in a final volume of 1 mL. Reactions were initiated with 10 U alcohol dehydrogenase (Cat. No. A3263, Sigma, prepared fresh 500 U/mL 100 mM Na-BICINE, pH 8.0, containing 1.0 mg/mL BSA). Initial velocity of MTT reduction was monitored at 570 nm at 37 °C. Amounts of NAD^+ and NADH were calculated by comparison to a standard curve of velocity vs NAD^+ over a range of 2.0–100 pmol NAD^+. Data were normalized to 10^6 cells and expressed as the mean ± standard deviation of three independent experiments.

Amounts of $NADP^+$ and NADPH were similarly measured in reactions containing pyridine nucleotide extractions in the presence of 2.5 mM G6P, 0.42 mM MTT, 1.66 mM PES, and 4.16 mM EDTA in 100 mM Na-BICINE buffer, pH 8.0, in a final volume of 1 mL. Following a 5 min preincubation at 37 °C, reactions were initiated with 0.7 U of G6PD (Cat. No. G4134, Sigma). Initial velocity of MTT reduction was monitored at 570 nm at 37 °C. Amounts of $NADP^+$ and NADPH were calculated by comparison to a standard curve of velocity vs $NADP^+$ over a range of 2.0–100 pmol of $NADP^+$. Data were normalized to 10^6 cells and expressed as the mean ± standard deviation of three independent experiments.

Real-Time RT-PCR. Real-time RT-PCR was used to compare transcript levels for P450 and AKR proteins involved in PAH *trans*-dihydrodiol metabolism in A549 cells. One microgram of total RNA was reverse-transcribed using the GeneAmp RNA PCR Core Kit (Applied Biosystems, Foster City, CA). Each plate contained nine full-length standards (0.025–2 500 000 fg) in duplicate and samples in triplicate. The amount of target cDNA was established through comparison of threshold cycle (C_T) values for each sample to a standard curve generated for each gene. Expression was normalized to the high abundance and low abundance housekeeping genes, for example, glyceraldehyde-3-phosphate dehydrogenase (GAPDH) and porphobilinogen deaminase (PBGD), respectively.

The primer sequences for PCR amplification of P450 1A1, P450 1B1, AKR1C1–1C4, GAPDH, and PBGD genes were obtained from previous publications (*42, 43*). The primers for AKR1A1 are forward, 5′-dTTA TGC CTT TGA GCG GGG AGA CA-3′, and reverse, 5′-dTTG AAG TTG GAC AGG CCC AGC G-3′, giving a 150 bp product. Quantitative analysis of the specific expression of each gene was performed on a DNA Engine thermal cycler (MJ Research, Waltham, MA) with SYBR Green detection. PCR conditions were as follows: 95 °C for 15 min followed by 40 cycles of 94 °C for 15 s of denaturation, *X* °C for 30 s for annealing, and 72 °C for 30 s for extension (where $X = 60$ °C for P450 1A1 and 1B1, 57 °C for AKR1C1, 60 °C for AKR1C2 and AKR1C3, 56 °C with addition of 4% DMSO for AKR1C4, 60 °C for AKR1A1, and 58 °C for GAPDH and PBGD). Specificity of P450 1A1 and 1B1 primers was validated with 2500 fg of full-length standard of the alternative isoform, and AKR primer specificity was confirmed with 2500 fg of full-length standards of each AKR isoform.

Full-length cDNA standards of P450 1A1 and 1B1 were generated from the prokaryotic expression vectors pCW containing the respective cDNA clones (*44, 45*) via digestion with *Nde*I and *Xba*I. cDNA standards for AKR1A1 and AKR1C1–1C4 were similarly prepared from their pET-16b vectors (*17, 38*) via digestion with either *Nco*I and *Bam*HI (AKR1A1) or *Xho*I and *Bgl*II (AKR1Cs). Standards for GAPDH and PBGD were generated by isolating the PCR product following PCR amplification of human kidney cDNA. Digestion products were isolated by gel purification and used as standards with correction factors for GAPDH (3.30) and PBGD (7.48) due to differences in molecular weight between full-length and PCR product standards.

Data were analyzed for significance using a one-way ANOVA test with Bonferroni post-hoc correction for multiple comparisons, using the statistical analysis program SigmaStat (Port Richmond, CA). Differences between AKR and P450 transcript levels following DMSO- or TCDD-treatment of A549 cells were considered significant at $P < 0.001$.

Functional Enzyme Assay. Cell lysates were prepared by scraping cells into 100 mM potassium phosphate buffer, pH 7.0, homogenizing them on ice with a Dounce homogenizer, and removing cell debris by centrifugation at 10 000 *g*. Cell lysates (100 μg/mL) were incubated at 25 °C in 100 mM potassium phosphate buffer, pH 7.0, with 1 mM *p*-nitrobenzaldehyde in 4% ACN and 180 μM NADPH to determine AKR1A1 activity. Consumption of NADPH was monitored spectrophotometrically at 340 nm. AKR1C activity was measured by oxidation of 200 μM 1-acenaphthenol (final 4% MeOH) at 25 °C in 100 mM potassium phosphate buffer, pH 7.0, containing 2.3 mM NAD^+. Production of NADH was monitored spectrophotometrically at 340 nm. Inhibition of AKR activity was achieved with 150 μM ponalrestat (AKR1A1 specific) or 100 μM flufenamic acid (AKR1C specific). P450 1A1/1B1 activity was measured by standard EROD assays containing 100 μg of cell lysate, 100 mM potassium phosphate, pH 7.4, an NADPH-regenerating system (as described above), and 1 μg of 7-ethoxyresorufin in a final volume of 1 mL. Production of resorufin was monitored fluorimetrically at 37 °C and quantitated by comparison to a standard curve of resorufin fluorescence ($\lambda_{ex} = 550$ nm, $\lambda_{em} = 586$ nm).

Results

***In Vitro* Kinetic Comparison of (±)-B[*a*]P-7,8-Diol Oxidation Catalyzed by P450 and AKR Enzymes.** We examined the kinetic constants for (±)-B[*a*]P-7,8-diol utilization catalyzed by human P450 1A1 and 1B1, AKR1A1, and AKR1C enzymes under identical conditions at physiological pH, using their preferred nicotinamide cofactors (NADPH for P450 isoforms and $NADP^+$ for AKR isoforms).

We determined the kinetic constants (k_{cat}, K_m, and k_{cat}/K_m) for the monooxygenation of (±)-B[*a*]P-7,8-diol catalyzed by P450 1A1 and 1B1. The rate of formation of *anti*-BPDE was measured by monitoring the disappearance of (±)-B[*a*]P-7,8-diol and the formation of (±)-B[*a*]P-tetraol 1, the major hydrolysis product of (±)-*anti*-BPDE (Figure 1A−C). The k_{cat} values were found to be 9.3 min^{-1} and 3.8 min^{-1} and K_m values were found to be 0.53 μM and 1.0 μM for P450 1A1 and 1B1, respectively, yielding k_{cat}/K_m values of 17 000 mM^{-1} min^{-1} and 3800 mM^{-1} min^{-1} for each enzyme (Figure 2).

We next determined the kinetic constants of (±)-B[*a*]P-7,8-diol oxidation catalyzed by human AKRs. For the AKR-mediated reactions, the disappearance of (±)-B[*a*]P-7,8-diol was followed over time. Excellent agreement was obtained between the rate of (±)-B[*a*]P-7,8-diol disappearance and the formation of B[*a*]P-7,8-dione, trapped as its thiol conjugate with β-mercaptoethanol. Quantitative trapping of B[*a*]P-7,8-dione under these conditions was previously verified using [^{3}H]-B[*a*]P-7,8-dione (*40*). Representative data are shown (Figure 1D−F).

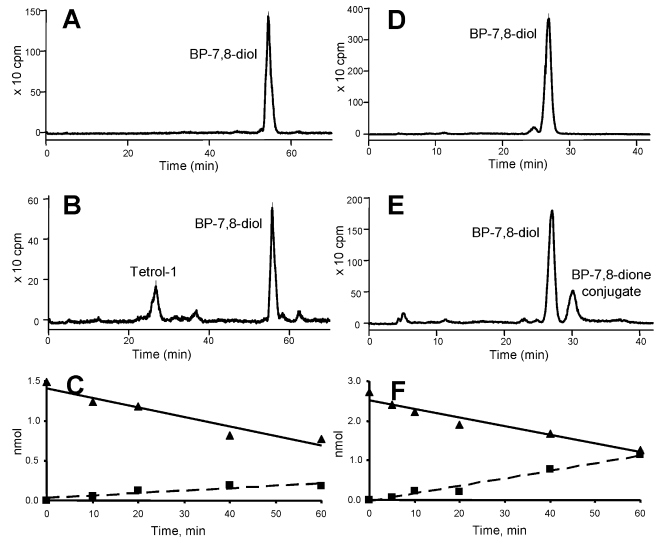

Figure 1. Metabolism of [^{3}H]-(±)-B[*a*]P-7,8-diol via P450 1A1 and AKR1C2. P450 1A1 oxidized 20 μM [^{3}H]-(±)-B[*a*]P-7,8-diol to form (±)-*anti*-BPDE, generating the major hydrolysis product (±)-B[*a*]P-tetraol 1 after 0 min (A) and 60 min (B). P450 1A1-catalyzed (±)-B[*a*]P-7,8-diol consumption (solid line) shows concomitant formation of (±)-B[*a*]P-tetraol 1 (dashed line) (C). AKR1C2 oxidized 20 μM [^{3}H]-(±)-B[*a*]P-7,8-diol to generate B[*a*]P-7,8-dione, trapped as a thioether conjugate with β-mercaptoethanol after 0 min (D) and 60 min (E). Initial rates of (±)-B[*a*]P-7,8-diol consumption (solid line) and B[*a*]P-7,8-dione conjugate formation (dashed line) indicate stoichiometric trapping of B[*a*]P-7,8-dione (F). Panels A, B, D, and E are radiochromatograms, and panels C and F are progress curves.

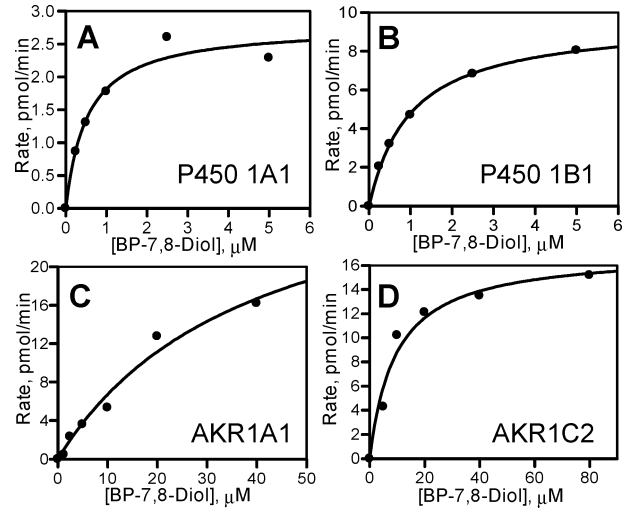

Figure 2. Determination of steady-state kinetic constants for oxidation of (±)-B[*a*]P-7,8-diol catalyzed by P450 1A1 (A), P450 1B1 (B), AKR1A1 (C), and AKR1C2 (D). End-point assays were performed in duplicate over 1 h, and (±)-B[*a*]P-7,8-diol consumption was measured by RP-HPLC. Plots of pmol/min (±)-B[*a*]P-7,8-diol consumed versus substrate concentration are shown.

The end point of the reaction for AKR1A1 comprised 50% of the (±)-B[*a*]P-7,8-diol since this enzyme is stereospecific for oxidation of the (−)-B[*a*]P-7,8-diol stereoisomer (*17*). For the AKR1C1–1C4 reactions, the end point of the reaction corresponded to 100% depletion of (±)-B[*a*]P-7,8-diol because both stereoisomers are utilized (*38*). The k_{cat} values ranged from 0.42 to 1.2 min^{-1}, and K_m values were found to be 39, 9.5, and 17 μM for AKR1A1, AKR1C2, and AKR1C3, respectively. AKR1C1 and AKR1C4 were not saturable due to the limited solubility of (±)-B[*a*]P-7,8-diol. Of the AKR enzymes examined, AKR1C2 and AKR1A1 had the highest catalytic efficiencies (k_{cat}/K_m) of 53 and 31 mM^{-1} min^{-1}, respectively, Table

Table 1. Steady-State Kinetic Parameters for Oxidation of (±)-B[*a*]P-7,8-diol Catalyzed by Human AKR and P450 Enzymes

enzyme	k_{cat}[a] (min^{-1})	K_m[a] (μM)	k_{cat}/K_m[a] (mM^{-1} min^{-1})
P450 1A1	9.3 ± 0.7	0.53 ± 0.14	17000 ± 1000
P450 1B1	3.8 ± 0.1	1.0 ± 0.1	3800 ± 100
AKR1A1	1.2 ± 0.3	39 ± 15	31 ± 7
AKR1C2	0.50 ± 0.04	9.5 ± 2.6	53 ± 4
AKR1C3	0.42 ± 0.03	17 ± 2	25 ± 2
enzyme	V_{max}/K_m[b] (nmol min^{-1} mM^{-1})		k_{cat}/K_m (mM^{-1} min^{-1})
AKR1C1	1.5 ± 0.1		23 ± 1
AKR1C4	0.89 ± 0.03		17 ± 1

[a] Values are mean ± standard error. [b] When [S] ≪ K_m, then $v/[S] \approx V_{max}/K_m$ to obtain an estimate of k_{cat}/K_m.

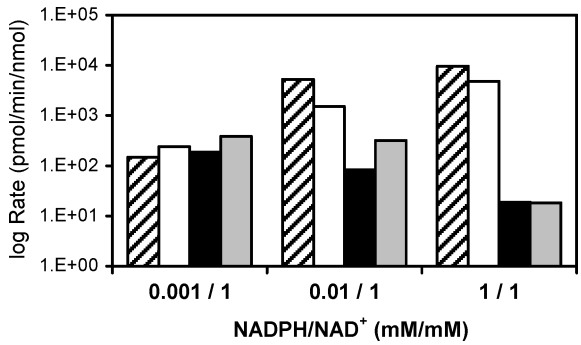

Figure 3. Cofactor ratios dictate rates of (±)-B[*a*]P-7,8-diol oxidation by P450 and AKR isoforms: P450 1A1 (hatched bars), P450 1B1 (white bars), AKR1A1 (black bars), and AKR1C2 (gray bars) were each incubated in duplicate with 10 μM (±)-B[*a*]P-7,8-diol in 50 mM MOPS buffer, pH 7.4, as the ratio of NADPH/NAD^+ cofactors was varied. The AKR pathway of (±)-B[*a*]P-7,8-diol metabolism favored lower NADPH concentrations, and P450 enzymes preferred higher NADPH concentrations.

1. P450 1B1 was 100-fold more catalytically efficient than the AKRs examined, and P450 1A1 was the most efficient enzyme studied, being approximately 500-fold more efficient than the AKR enzymes in the activation of (±)-B[*a*]P-7,8-diol under these conditions.

Effect of Cofactor Ratio on the Favored Pathway of (±)-B[*a*]P-7,8-Diol Activation. The kinetic constants reported were obtained under optimal cofactor conditions, using an NADPH-regenerating system for P450 isoforms and $NADP^+$ for AKR isoforms. These do not reflect the true cofactor concentrations that these enzymes would be exposed to in the cell. While NADPH is the major reductive cofactor, P450 isozymes are not linked to an NADPH-regenerating system. Moreover, NAD^+ rather than $NADP^+$ is the major oxidative cofactor in the cell (*46*). To ascertain the effect of cofactor composition on the preferred metabolic pathway of PAH *trans*-dihydrodiol oxidation, we varied the molar ratio of NADPH/NAD^+ from 0.001 to 1.0 and measured the specific activity of (±)-B[*a*]P-7,8-diol oxidation. This was achieved by varying NADPH from 0.001 to 1.0 mM while holding NAD^+ constant at 1.0 mM, Figure 3. At a molar ratio of 1:1000 (0.001 mM NADPH/1 mM NAD^+) it was found that P450 and AKR isoforms perform equally well in the metabolism of (±)-B[*a*]P-7,8-diol. Increasing NADPH concentrations to a molar ratio of 1:100 (0.01 mM NADPH/1 mM NAD^+) favored the P450 activity by approximately 40-fold, and when equimolar concentrations (1 mM NADPH/1 mM NAD^+) were used, the P450 pathway was favored by 400-fold.

Nicotinamide Adenine Dinucleotide Levels in A549 Cells. We next measured NAD(H) and NADP(H) in A549 cells to determine basal cofactor levels using enzymatic cycling methods (Table 2). NAD^+ was the major oxidative cofactor in A549 cells (450 ± 50 pmol $NAD^+/10^6$ cells versus 33 ± 9 pmol $NADP^+/10^6$ cells). Concentrations of the reductive cofactors NADH and NADPH were comparable (150 ± 20 pmol NADH/10^6 cells and 130 ± 20 pmol NADPH/10^6 cells). The NADPH/NAD^+ ratio (0.28) in A549 cells was of interest for comparison to our *in vitro* data on the effect of cofactor levels on the preferred pathway of (±)-B[*a*]P-7,8-diol metabolism. These data suggest that basal levels of NADPH/NAD^+ would favor the P450 pathway by 100-fold if P450 and AKR isoforms are equally expressed.

Table 2. Nicotinamide Adenine Dinucleotide Cofactor Concentrations in A549 Cells

cofactor	pmol/10^6 cells	ratio
NADH	150 ± 20	
NAD^+	450 ± 50	
NADH/NAD^+		0.32
NADPH	130 ± 20	
$NADP^+$	33 ± 9	
NADPH/$NADP^+$		4.0
NADPH/NAD^+		0.28

Real-Time RT-PCR. To determine whether the P450 or AKR pathway predominates in A549 cells, expression of mRNA transcripts was evaluated in A549 cells by real-time RT-PCR (Figure 4). Transcript levels were normalized to the high-abundance housekeeping gene GAPDH. Results were comparable when normalized to the low-abundance housekeeping gene PBGD (data not shown). Basal expression of P450 1A1 was not detected but was induced following 12 h treatment with 10 nM of the AhR-agonist TCDD (Figure 4A). P450 1B1 transcript levels were expressed at basal levels similar to those seen for P450 1A1 in TCDD-induced cells and were also inducible by TCDD (5.2-fold).

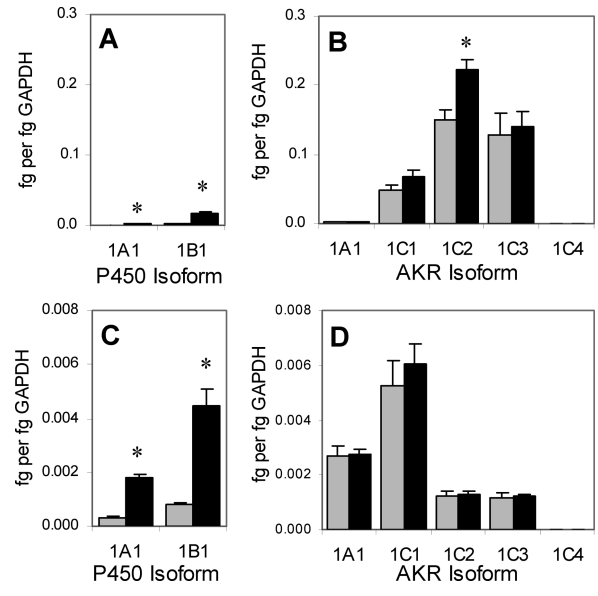

Figure 4. Expression of transcripts involved in metabolic activation of PAH *trans*-dihydrodiols in A549 human lung adenocarcinoma and HBEC-KT immortalized normal human bronchial epithelial cells. mRNA levels of P450 (A, C) and AKR (B, D) transcripts were evaluated using real-time RT-PCR analysis of A549 (A, B) and HBEC-KT (C, D) cells following 12 h treatment with 0.1% DMSO (gray bars) or 10 nM TCDD (black bars). Notice that the scale of the *y* axis is different in (C, D). Each real-time experiment was performed in triplicate with the mean and standard deviation shown. Data were normalized to the GAPDH housekeeping gene. Asterisk indicates statistically different expression between DMSO- and TCDD-treated samples with p values of $P < 0.001$ defining significance.

Table 3. Functional Enzyme Assays in A549 Cells

enzyme	functional assay	purified protein,[a] nmol min^{-1} mg^{-1}	A549 cell lysate, nmol min^{-1} mg^{-1}	HBEC-KT cell lysate, nmol min^{-1} mg^{-1}
AKR1A1	*p*-nitrobenzaldehyde reduction, 1 mM	6000	50.1 ± 2.8	15.7 ± 3.9
AKR1C1−1C3	1-acenaphthenol oxidation, 200 μM	2100–2800	30.4 ± 2.2	0.58 ± 0.07
P450 1A1	ethoxyresorufin O^7-deethylation, 4.1 μM	2.6	N.D.[b]	*b*
P450 1B1	ethoxyresorufin O^7-deethylation, 4.1 μM	1.2	*b*	*b*

[a] Purified AKRs, P450 Supersomes. [b] Not detectable.

AKR1A1 mRNA transcripts were minimally expressed in A549 cells (Figure 4B). AKR1C4 expression was not detected, as expected for this liver-specific gene (*47*). Of the remaining AKR1Cs, AKR1C2 was the dominant transcript expressed, although AKR1C1 and AKR1C3 transcript levels were significant. AKR1C2 mRNA appeared weakly inducible with TCDD (less than 2-fold, $P < 0.001$), despite the absence of an XRE in the promoter region of this gene (*48*), indicating potential regulation via an indirect TCDD-mediated mechanism. By contrast, transcript levels of AKR1C1 and AKR1C3 were not affected by TCDD. mRNA levels for AKR1C2 and AKR1C3 were 91- and 58-fold greater than P450 1A1 transcript levels following TCDD treatment ($P < 0.001$). mRNA levels for AKR1C2 and AKR1C3 were 13- and 8-fold greater than P450 1B1 transcript levels following TCDD-induced A549 cells ($P < 0.001$). These real-time RT-PCR data indicate dominant expression of AKR1C transcripts when compared with both basal and TCDD-induced P450 1A1 and 1B1.

Transcript levels of P450 and AKR isoforms were also evaluated in HBEC-KT cells to determine their levels in immortalized normal human lung epithelial cells (Figure 4C). P450 1A1 was expressed at similar levels in A549 and HBEC-KT cells following 12 h treatment with 10 nM TCDD. Basal P450 1B1 transcript levels were 4.2-fold lower in HBEC-KT cells than in A549 cells. Fold induction of P450 1B1 expression was similar in both human lung cell lines.

AKR1A1 mRNA transcripts were expressed in HBEC-KT cells at levels similar to those in A549 cells (Figure 4D). AKR1C4 was also not detected in these cells. AKR1C transcripts were generally expressed at significantly lower levels in HBEC-KT cells when compared with A549 cells. AKR1C1 was the dominant AKR1C transcript in HBEC-KT cells, a striking difference from A549 cells where AKR1C2 and AKR1C3 were the most prevalent of the AKRs expressed. AKR1C1 transcript levels were approximately 10-fold lower in HBEC-KT cells than in A549 cells. AKR1C2 and AKR1C3 transcript levels were 120- and 110-fold lower in HBEC-KT cells than in A549 cells, respectively. Up-regulation of AKR expression with TCDD treatment was not observed in HBEC-KT cells.

Relative transcript levels of P450 and AKR isoforms were more similar in HBEC-KT cells than in A549 cells. In HBEC-KT cells, basal levels of AKRs exceeded P450 1A1 transcript levels by 3.4- to 15-fold and exceeded P450 1B1 transcript levels by 1.4- to 6.5-fold. Induction of P450 1A1 with 10 nM TCDD for 12 h resulted in mRNA transcripts approximately 1.5-fold greater than AKR1C2 and AKR1C3, 1.5-fold less than AKR1A1, and 2.9-fold less than AKR1C1. Induction of P450 1B1 resulted in mRNA transcript levels that were up to 3.9-fold greater than AKR1A1, AKR1C2, and AKR1C3; TCDD-induced P450 1B1 transcript levels were comparable with those of AKR1C2 in HBEC-KT cells.

Enzyme Assays in Cells. Our studies indicate that the preferred pathway of (±)-B[*a*]P-7,8-diol oxidation will depend upon redox state and enzyme expression levels. To assess functional enzyme expression, enzyme activity measurements were also performed. Reduction of 1 mM *p*-nitrobenzaldehyde in A549 cell lysates was measured to determine AKR1A1 functional activity (6.0 μmol min^{-1} mg^{-1} purified AKR1A1) and an initial velocity of 50.1 nmol min^{-1} mg^{-1} total protein was observed (*17*), Table 3. This activity was inhibited 43% by 150 μM ponalrestat, an AKR1A1 inhibitor (data not shown). AKR1A1 functional activity in HBEC-KT cells (50.7 nmol min^{-1} mg^{-1}) was comparable to that in A549 cells and was also inhibited by ponalrestat. Oxidation of 200 μM 1-acenaphthenol (2.1–2.8 μmol min^{-1} mg^{-1} purified AKR1C1−AKR1C3) proceeded in A549 lysates at a rate of 30.4 nmol min^{-1} mg^{-1} and was abrogated with 100 μM flufenamic acid, an AKR1C inhibitor (data not shown) (*18*). AKR1C functional activity in HBEC-KT cells (0.58 nmol min^{-1} mg^{-1}) was 50-fold lower than that in A549 cells where the limit of detection is 159 pmol min^{-1}. EROD activity was not detected in lysates from either DMSO- or 10 nM TCDD-treated A549 or HBEC-KT cells, indicating a lack of functional P450 1A1 and 1B1 expression. By contrast, the EROD assay detected robust P450 1A1/1B1 activity in TCDD-treated human HepG2 cells yielding a specific activity of 6.7 pmol min^{-1} mg^{-1} cell lysate (data not shown), consistent with previously reported values (*49*). It is estimated that the limit of sensitivity of this assay is 0.5 pmol min^{-1}, suggesting that the level of P450 activity corresponds to less than 0.04 μg per 100 μg of cell lysate.

Discussion

This study constitutes the first *in vitro* comparison of P450 and AKR pathways in the metabolic activation of proximate carcinogen PAH *trans*-dihydrodiols. In previous studies, kinetic constants for oxidation of (±)-B[*a*]P-7,8-diol by P450 1A1 and 1B1 were reported (*8, 50–54*); our data are in agreement with these values. In addition, prior measurements of AKR-mediated PAH *trans*-dihydrodiol metabolism were performed at pH 9.0 to favor oxidation (*17, 18, 38*). Kinetic values were thus determined at pH 7.4 to attain physiological relevance and for direct comparison with P450 enzymes. Values of k_{cat} did not vary greatly between P450 and AKR enzymes, demonstrating that K_m values largely dictate the enhanced monooxygenation of (±)-B[*a*]P-7,8-diol by P450 enzymes over the oxidation of (±)-B[*a*]P-7,8-diol by AKR isoforms. Our data indicate that P450 1A1 and 1B1 are 500- and 100-fold more catalytically efficient than AKR isoforms in the consumption of (±)-B[*a*]P-7,8-diol substrate.

Initial rates of (±)-B[*a*]P-7,8-diol oxidation were measured for P450 1A1, P450 1B1, AKR1A1, and AKR1C2 as the ratio of NADPH/NAD$^+$ cofactors was varied to determine the redox state necessary for AKRs to successfully compete for *trans*-dihydrodiols. NADPH is the cofactor utilized by P450s for monooxygenation of PAH *trans*-dihydrodiols. AKRs may employ either NAD$^+$ or NADP$^+$ cofactors in PAH *trans*-dihydrodiol oxidation. However, their affinity for NADP$^+$ is 100- to 1000-fold greater than for NAD$^+$ (*55*). We find that low NADPH/NAD$^+$ molar ratios (1:1000) facilitate (±)-B[*a*]P-7,8-diol oxidation via both P450 and AKR pathways. Preference

for the P450 pathway is attained as the concentration of NADPH is increased relative to NAD^+.

In rat liver cytosol, there is general consensus that [NAD^+] ≫ [NADH] and [NADPH] ≫ [$NADP^+$] (*46*), with the total concentration of NAD(H) exceeding that of NADP(H) by approximately 10-fold (*56*). However, concentrations of nicotinamide adenine dinucleotide cofactors in human tissues have not been widely determined. Measurement of the major oxidative and reductive cofactors, NAD^+ and NADPH, in both human red blood cells and a human leukemic monocytic cell line yielded a NADPH/NAD^+ ratio of approximately 0.3 (*57–59*). We measured NAD(H) and NADP(H) concentrations in A549 cells, a relevant human lung cell line. Our data are in concordance with NAD^+ ≫ NADH and NADPH ≫ $NADP^+$, and total NAD(H) is 4-fold greater than total NADP(H). Additionally, the NADPH/NAD^+ ratio was found to be 0.28. This value indicates that the redox state of basal A549 cells will favor metabolism of (±)-B[*a*]P-7,8-diol via P450 1A1 and 1B1 by about 100-fold. However, the very formation of redox-active PAH *o*-quinones by AKRs can lead to futile redox-cycling and an altered redox state that would favor the AKR pathway (*23*).

We next measured enzyme expression levels in A549 human lung adenocarcinoma cells. Expression of AKR1C1−AKR1C3 was previously documented in these cells at both the mRNA and functional level, and cell lysates were able to oxidize DMBA-3,4-diol to DMBA-3,4-dione (*18*). Analysis of mRNA transcript levels revealed induction of P450 1A1 with the AhR agonist TCDD; however, the abundance of the induced transcripts was relatively low. P450 1B1 mRNA was nominally expressed at a basal level and was weakly inducible with TCDD treatment. Expression of AKR1C1−AKR1C3 mRNA transcripts greatly exceeded those of P450 1A1 and 1B1. For example, AKR1C2 was expressed at levels 90- and 13-fold greater than the levels of P450 1A1 and 1B1, respectively, in TCDD-treated cells.

A549 cells have been used to study induction of P450 enzymes but may not be an ideal system to extrapolate relative expression of enzyme isoforms to human lung, because significant genetic changes may accompany transformation. HBEC-KT cells were used as a model system for normal human bronchial epithelial cells. These cells were generated by nonviral immortalization of a lung cancer-free human bronchial epithelial biopsy specimen through expression of hTERT and Cdk4 genes (*37*). Analysis of mRNA transcripts revealed a universally lower expression of AKR1Cs in HBEC-KT cells compared with that in A549 cells. Contrary to A549 cells, which have dominant AKR1C2 and AKR1C3 expression, AKR1C1 was the dominant AKR1C transcript in HBEC-KT cells. Basal levels of P450 1B1 transcripts were lower in HBEC-KT than in A549 cells; however, induction with TCDD was comparable between the two cell types. These data indicate that transformation of human bronchial epithelial cells is accompanied by an up-regulation of AKR1Cs, particularly AKR1C2 and AKR1C3, as well as basal levels of P450 1B1. Despite the significantly lower levels of AKRs expressed in a cell line more closely resembling normal bronchial epithelium compared with those in A549 cells, the expression of multiple AKRs are likely to generate an environment where total basal AKR expression exceeds that of P450 expression in human lung.

Our data are consistent with reports that P450 1A1 mRNA is not commonly expressed in human lung and P450 1B1 is expressed at basal levels (*7, 60*). Real-time RT-PCR technology has allowed improved quantitation of basal and induced P450 1A1 and 1B1 mRNA in A549 cells. Following B[*a*]P or TCDD treatment, induction of P450 1A1 and 1B1 transcripts was reported up to 13- and 3.6-fold, respectively (*36, 61*). Low levels of these P450 isoforms should not be interpreted to mean that activation of PAHs by P450 isoforms does not occur. A549 cells treated with B[*a*]P form BPDE−DNA adducts (*62*). Additionally, B[*a*]P-tetraols are detected in A549 cells treated with (±)-B[*a*]P-7,8-diol by LC/MS, indicating P450-mediated generation of BPDE.[2]

P450 isoforms other than P450 1A1 and 1B1 may also be responsible for the metabolic activation of B[*a*]P-7,8-dihydrodiol. Recent studies by us in human bronchoalveolar H358 cells showed that levels of (+)-*trans*-*anti*-BPDE−N^2-dGuo adducts were greater in cells in which P450 1A1/1B1 were uninduced and that their induction led to a diminution in DNA adducts (*9*). In addition, H358 cells have sufficient peroxidase activity to activate B[*a*]P to radical cation metabolites, B[*a*]P-1,6-dione and B[*a*]P-3,6-dione, in the absence of induced P450 isoforms (*63*).

We also measured P450 and AKR isoforms in the two cell lines by functional enzyme assay. Despite several reports of TCDD-inducible P450 1A1/1B1 expression in A549 cells (*35, 36, 64*), lysates from these cells did not demonstrate functional P450 1A1/1B1 expression using standard EROD assays. Functional P450 1A1/1B1 expression was similarly not detected in HBEC-KT cell lysates. We conclude that, while induction of both isoforms is evident at the mRNA level, protein levels are insufficient for detection of activity by standard enzyme assay where the limit of detection is 0.5 pmol min^{-1}. We confirmed robust functional AKR1C expression in A549 cells by measuring the oxidation of 1-acenaphthenol. These cells were also able to rapidly reduce *p*-nitrobenzaldehyde despite minimal levels of AKR1A1 transcripts; other AKR isoforms, including AKR1B1, may be responsible for this activity (*65*). Expression of functional AKR1C was significantly lower in HBEC-KT than in A549 cells, in concordance with real-time RT-PCR data of mRNA expression, but still detectable by measuring the oxidation of 1-acenaphthenol. *p*-Nitrobenzaldehyde reductase activity in HBEC-KT and A549 cells was similar. All the AKR assays measure the change in NAD(P)H concentration spectrophotometically where the limit of detection is 159 pmol min^{-1}. The ability to detect functional AKR activity but not functional P450 activity in both cell lines, when the EROD assay is 300-fold more sensitive, suggests that the expression of AKR enzymes is sufficient to impact PAH *trans*-dihydrodiol metabolism.

The ability to detect AKR activity in the absence of P450 activity when their transcript levels are similar in HBEC-KT cells requires comment in light of the greater sensitivity of the P450 assay. There are several reasons why transcript levels may not reflect activity measurements. These include post-transcriptional regulation of expression, post-translational regulation of expression, or limiting amounts of NADPH-P450 oxidoreductase. Of these, the former seems a possibility since immunoblots of P450 1A1 or 1B1 expression in HBEC-KT cells were negative (data not shown).

Extensive *trans*-dihydrodiol metabolism by AKR enzymes may not be necessary for PAH *o*-quinones to exert their detrimental effects. Generation of ROS by PAH *o*-quinones has been well-documented and may lead to oxidative stress (*23–27*). Cellular response to oxidative stress comprises transcription of genes containing an antioxidant response element (ARE) in their promoter region, including UDP-glycosyltransferases and NAD-

[2] Park, J. H., Mangal, D., Tacka, K. A., Quinn, A. M., Harvey, R. G., Blair, I. A., and Penning, T. M. Unpublished data.

(P)H-quinone oxidoreductase 1. In fact, AKR1Cs are up-regulated in response to oxidative stress via an ARE-dependent pathway (*66, 67*). Generation of redox-active PAH *o*-quinones thus produces two signals that would exacerbate the AKR pathway. Redox-cycling could deplete NADPH and generate a redox-state that favors the AKR pathway, while concomitant generation of ROS during redox-cycling could lead to AKR1C induction via the ARE.

Given the scheme of PAH metabolism involving induction, inhibition, and cross-talk between enzyme pathways, it is difficult to ascertain the precise contribution of P450 and AKR isoforms to smoking-induced lung carcinogenesis. Clearly, their roles in PAH activation will depend on the relative expression of these enzymes, their induction, and the redox state of PAH-exposed lung cells. The P450 pathway of PAH metabolism is widely accepted, and (±)-*anti*-BPDE is considered the ultimate carcinogen of B[*a*]P. Here we present evidence that the human AKR enzymes may also be key players in the activation of PAH *trans*-dihydrodiols through their ability to generate reactive and redox-active *o*-quinones. Functional expression levels are sufficient in human lung adenocarcinoma A549 cells and immortalized normal human bronchial epithelial HBEC-KT cells to successfully compete with P450 1A1 and 1B1 for carcinogenic activation of (±)-B[*a*]P-7,8-diol. In further support of this contention, using A549 cells treated with (±)-B[*a*]P-7,8-diol, we have observed AKR-mediated B[*a*]P-7,8-dione formation, intracellular ROS formation, and increases in 8-oxo-dGuo (*68*).

Acknowledgment. This work was supported by NIH Grants P01 CA092537, R01 CA39504, and P30 ES013508.

References

(1) IARC (1983) IARC Monographs on the Evaluation of the Carcinogenic Risk of Chemicals to Humans, Polynuclear Aromatic Compounds, Part I, Chemical, Environmental, and Experimental Data, Vol. 32, IARC, Lyon, France.

(2) Straif, K., Baan, R., Grosse, Y., Secretan, B., El Ghissassi, F., and Cogliano, V. (2005) Carcinogenicity of polycyclic aromatic hydrocarbons. *Lancet Oncol. 6*, 931–932.

(3) Cavalieri, E. L., and Rogan, E. G. (1995) Central role of radical cations in metabolic activation of polycyclic aromatic hydrocarbons. *Xenobiotica 25*, 677–688.

(4) Jeffrey, A. M., Jennette, K. W., Blobstein, S. H., Weinstein, I. B., Beland, F. A., Harvey, R. G., Kasai, H., Miura, I., and Nakanishi, K. (1976) Benzo[a]pyrene-nucleic acid derivative found *in vivo*: structure of a benzo[*a*]pyrenetetrahydrodiol epoxide-guanosine adduct. *J. Am. Chem. Soc. 98*, 5714–5715.

(5) Koreeda, M., Moore, P. D., Wislocki, P. G., Levin, W., Yagi, H., and Jerina, D. M. (1978) Binding of benzo[*a*]pyrene 7,8-diol-9,10-epoxides to DNA, RNA, and protein of mouse skin occurs with high stereoselectivity. *Science 199*, 778–781.

(6) Conney, A. H. (1982) Induction of microsomal enzymes by foreign chemicals and carcinogenesis by polycyclic aromatic hydrocarbons: G. H. A. Clowes Memorial Lecture. *Cancer Res. 42*, 4875–4917.

(7) Shimada, T., Hayes, C. L., Yamazaki, H., Amin, S., Hecht, S. S., Guengerich, F. P., and Sutter, T. R. (1996) Activation of chemically diverse procarcinogens by human cytochrome P-450 1B1. *Cancer Res. 56*, 2979–2984.

(8) Kim, J. H., Stansbury, K. H., Walker, N. J., Trush, M. A., Strickland, P. T., and Sutter, T. R. (1998) Metabolism of benzo[a]pyrene and benzo[a]pyrene-7,8-diol by human cytochrome P450 1B1. *Carcinogenesis 19*, 1847–1853.

(9) Ruan, Q., Gelhaus, S. L., Penning, T. M., Harvey, R. G., and Blair, I. A. (2007) Aldo-keto reductase- and cytochrome P450-dependent formation of benzo[*a*]pyrene-derived DNA adducts in human bronchoalveolar cells. *Chem. Res. Toxicol. 20*, 424–431.

(10) Tretyakova, N., Matter, B., Jones, R., and Shallop, A. (2002) Formation of benzo[*a*]pyrene diol epoxide-DNA adducts at specific guanines within *K-ras* and *p53* gene sequences: stable isotope-labeling mass spectrometry approach. *Biochemistry 41*, 9535–9544.

(11) Zhang, Y., Wu, X., Guo, D., Rechkoblit, O., Geacintov, N. E., and Wang, Z. (2002) Two-step error-prone bypass of the (+)- and (−)-*trans-anti*-BPDE-N^2-dG adducts by human DNA polymerases η and κ. *Mutat. Res. 510*, 23–35.

(12) Tang, Y. M., Chen, G. F., Thompson, P. A., Lin, D. X., Lang, N. P., and Kadlubar, F. F. (1999) Development of an antipeptide antibody that binds to the C-terminal region of human CYP1B1. *Drug Metab. Dispos. 27*, 274–280.

(13) Whitlock, J. P. (1999) Induction of cytochrome P4501A1. *Annu. Rev. Pharmacol. Toxicol. 39*, 103–125.

(14) Mollerup, S., Ovrebo, S., and Haugen, A. (2001) Lung carcinogenesis: Resveratrol modulates the expression of genes involved in the metabolism of PAH in human bronchial epithelial cells. *Int. J. Cancer 92*, 18–25.

(15) Willey, J. C., Coy, E. L., Frampton, M. W., Torres, A., Apostolakos, M. J., Hoehn, G., Schuermann, W. H., Thilly, W. G., Olson, D. E., Hammersley, J. R., Crespi, C. L., and Utell, M. J. (1997) Quantitative RT-PCR measurement of cytochromes p450 1A1, 1B1, and 2B7, microsomal epoxide hydrolase, and NADPH oxidoreductase expression in lung cells of smokers and nonsmokers. *Am. J. Respir. Cell Mol. Biol. 17*, 114–124.

(16) Kim, J. H., Sherman, M. E., Curriero, F. C., Guengerich, F. P., Strickland, P. T., and Sutter, T. R. (2004) Expression of cytochromes P450 1A1 and 1B1 in human lung from smokers, non-smokers, and ex-smokers. *Toxicol. Appl. Pharmacol. 199*, 210–219.

(17) Palackal, N. T., Burczynski, M. E., Harvey, R. G., and Penning, T. M. (2001) The ubiquitous aldehyde reductase (AKR1A1) oxidizes proximate carcinogen *trans*-dihydrodiols to *o*-quinones: Potential role in polycyclic aromatic hydrocarbon activation. *Biochemistry 40*, 10901–10910.

(18) Palackal, N. T., Lee, S. H., Harvey, R. G., Blair, I. A., and Penning, T. M. (2002) Activation of polycyclic aromatic hydrocarbon *trans*-dihydrodiol proximate carcinogens by human aldo-keto reductase (AKR1C) enzymes and their functional overexpression in human lung carcinoma (A549) cells. *J. Biol. Chem. 277*, 24799–24808.

(19) Shou, M., Harvey, R. G., and Penning, T. M. (1993) Reactivity of benzo[*a*]pyrene-7,8-dione with DNA: evidence for the formation of deoxyguanosine adducts. *Carcinogenesis 14*, 475–482.

(20) McCoull, K. D., Rindgen, D., Blair, I. A., and Penning, T. M. (1999) Synthesis and characterization of polycyclic aromatic hydrocarbon *o*-quinone depurinating N^7-guanine adducts. *Chem. Res. Toxicol. 12*, 237–246.

(21) Balu, N., Padgett, W. T., Lambert, G. R., Swank, A. E., Richard, A. M., and Nesnow, S. (2004) Identification and characterization of novel stable deoxyguanosine and deoxyadenosine adducts of benzo[*a*]pyrene-7,8-quinone from reactions at physiological pH. *Chem. Res. Toxicol. 17*, 827–838.

(22) Balu, N., Padgett, W. T., Nelson, G. B., Lambert, G. R., Ross, J. A., and Nesnow, S. (2006) Benzo[*a*]pyrene-7,8-quinone-3′-mononucleotide adduct standards for ^{32}P postlabeling analyses: Detection of benzo[*a*]pyrene-7,8-quinone-calf thymus DNA adducts. *Anal. Biochem. 355*, 213–223.

(23) Flowers-Geary, L., Harvey, R. G., and Penning, T. M. (1993) Cytotoxicity of polycyclic aromatic hydrocarbon *o*-quinones in rat and human hepatoma cells. *Chem. Res. Toxicol. 6*, 252–260.

(24) Flowers, L., Bleczinski, W. F., Burczynski, M. E., Harvey, R. G., and Penning, T. M. (1996) Disposition and biological activity of benzo[*a*]pyrene-7,8-dione: A genotoxic metabolite generated by dihydrodiol dehydrogenase. *Biochemistry 35*, 13664–13672.

(25) Flowers, L., Ohnishi, S. T., and Penning, T. M. (1997) DNA strand scission by polycyclic aromatic hydrocarbon *o*-quinones: role of reactive oxygen species, Cu(II)/Cu(I) redox cycling, and *o*-semiquinone anion radicals. *Biochemistry 36*, 8640–8648.

(26) Park, J. H., Gopishetty, S., Szewczuk, L. M., Troxel, A. B., Harvey, R. G., and Penning, T. M. (2005) Formation of 8-oxo-7,8-dihydro-2′-deoxyguanosine (8-oxo-dGuo) by PAH *o*-quinones: involvement of reactive oxygen species and copper(II)/copper(I) redox cycling. *Chem. Res. Toxicol. 18*, 1026–1037.

(27) Park, J. H., Troxel, A. B., Harvey, R. G., and Penning, T. M. (2006) Polycyclic aromatic hydrocarbon (PAH) *o*-quinones produced by the aldo-keto-reductases (AKRs) generate abasic sites, oxidized pyrimidines, and 8-oxo-dGuo via reactive oxygen species. *Chem. Res. Toxicol. 19*, 719–728.

(28) Hainaut, P., and Pfeifer, G. P. (2001) Patterns of p53 G→T transversions in lung cancers reflect the primary mutagenic signature of DNA-damage by tobacco smoke. *Carcinogenesis 22*, 367–374.

(29) Shen, Y. M., Troxel, A. B., Vedantam, S., Penning, T. M., and Field, J. (2006) Comparison of p53 mutations induced by PAH *o*-quinones with those caused by *anti*-benzo[*a*]pyrene diol epoxide *in vitro*: role of reactive oxygen and biological selection. *Chem. Res. Toxicol. 19*, 1441–1450.

(30) Hsu, N. Y., Ho, H. C., Chow, K. C., Lin, T. Y., Shih, C. S., Wang, L. S., and Tsai, C. M. (2001) Overexpression of dihydrodiol dehydrogenase as a prognostic marker of non-small cell lung cancer. *Cancer Res. 61*, 2727–2731.

(31) Kazemi-Noureini, S., Colonna-Romano, S., Ziaee, A. A., Malboobi, M. A., Yazdanbod, M., Setayeshgar, P., and Maresca, B. (2004) Differential gene expression between squamous cell carcinoma of esophageus and its normal epithelium; altered pattern of mal, akr1c2, and rab11a expression. *World J. Gastroenterol. 10*, 1716–1721.

(32) Fukumoto, S., Yamauchi, N., Moriguchi, H., Hippo, Y., Watanabe, A., Shibahara, J., Taniguchi, H., Ishikawa, S., Ito, H., Yamamoto, S., Iwanari, H., Hironaka, M., Ishikawa, Y., Niki, T., Sohara, Y., Kodama, T., Nishimura, M., Fukayama, M., Dosaka-Akita, H., and Aburatani, H. (2005) Overexpression of the aldo-keto reductase family protein AKR1B10 is highly correlated with smokers' non-small cell lung carcinomas. *Clin. Cancer Res. 11*, 1776–1785.

(33) Woenckhaus, M., Klein-Hitpass, L., Grepmeier, U., Merk, J., Pfeifer, M., Wild, P., Bettstetter, M., Wuensch, P., Blaszyk, H., Hartmann, A., Hofstaedter, F., and Dietmaier, W. (2006) Smoking and cancer-related gene expression in bronchial epithelium and non-small-cell lung cancers. *J. Pathol. 210*, 192–204.

(34) Lieber, M., Smith, B., Szakal, A., Nelson-Rees, W., and Todaro, G. (1976) A continuous tumor-cell line from a human lung carcinoma with properties of type II alveolar epithelial cells. *Int. J. Cancer 17*, 62–70.

(35) Hukkanen, J., Lassila, A., Paivarinta, K., Valanne, S., Sarpo, S., Hakkola, J., Pelkonen, O., and Raunio, H. (2000) Induction and regulation of xenobiotic-metabolizing cytochrome P450s in the human A549 lung adenocarcinoma cell line. *Am. J. Respir. Cell Mol. Biol. 22*, 360–366.

(36) Martinez, J. M., Afshari, C. A., Bushel, P. R., Masuda, A., Takahashi, T., and Walker, N. J. (2002) Differential toxicogenomic responses to 2,3,7,8-tetrachlorodibenzo-*p*-dioxin in malignant and nonmalignant human airway epithelial cells. *Toxicol. Sci. 69*, 409–423.

(37) Ramirez, R. D., Sheridan, S., Girard, L., Sato, M., Kim, Y., Pollack, J., Peyton, M., Zou, Y., Kurie, J. M., Dimaio, J. M., Milchgrub, S., Smith, A. L., Souza, R. F., Gilbey, L., Zhang, X., Gandia, K., Vaughan, M. B., Wright, W. E., Gazdar, A. F., Shay, J. W., and Minna, J. D. (2004) Immortalization of human bronchial epithelial cells in the absence of viral oncoproteins. *Cancer Res. 64*, 9027–9034.

(38) Burczynski, M. E., Harvey, R. G., and Penning, T. M. (1998) Expression and characterization of four recombinant human dihydrodiol dehydrogenase isoforms: oxidation of *trans*-7,8-dihydroxy-7,8-dihydrobenzo[*a*]pyrene to the activated *o*-quinone metabolite benzo[*a*]pyrene-7,8-dione. *Biochemistry 37*, 6781–6790.

(39) Whalen, D. L., Montemarano, J. A., Thakker, D. R., Yagi, H., and Jerina, D. M. (1977) Changes of mechanisms and product distributions in the hydrolysis of benzo[*a*]pyrene-7,8-diol 9,10-epoxide metabolites induced by changes in pH. *J. Am. Chem. Soc. 99*, 5522–5524.

(40) Jiang, H., Shen, Y. M., Quinn, A. M., and Penning, T. M. (2005) Competing roles of cytochrome P450 1A1/1B1 and aldo-keto reductase 1A1 in the metabolic activation of (±)-7,8-dihydroxy-7,8-dihydrobenzo[*a*]pyrene in human bronchoalveolar cell extracts. *Chem. Res. Toxicol. 18*, 365–374.

(41) Jacobson, E. L., and Jacobson, M. K. (1976) Pyridine nucleotide levels as a function of growth in normal and transformed 3T3 cells. *Arch. Biochem. Biophys. 175*, 627–634.

(42) Bauman, D. R., Steckelbroeck, S., Peehl, D. M., and Penning, T. M. (2006) Transcript profiling of the androgen signal in normal prostate, benign prostatic hyperplasia, and prostate cancer. *Endocrinology 147*, 5806–5816.

(43) Berge, G., Mollerup, S., Ovrebo, S., Hewer, A., Phillips, D. H., Eilertsen, E., and Haugen, A. (2004) Role of estrogen receptor in regulation of polycyclic aromatic hydrocarbon metabolic activation in lung. *Lung Cancer 45*, 289–297.

(44) Parikh, A., Gillam, E. M., and Guengerich, F. P. (1997) Drug metabolism by *Escherichia coli* expressing human cytochromes P450. *Nat. Biotechnol. 15*, 784–788.

(45) Shimada, T., Wunsch, R. M., Hanna, I. H., Sutter, T. R., Guengerich, F. P., and Gillam, E. M. (1998) Recombinant human cytochrome P450 1B1 expression in *Escherichia coli*. *Arch. Biochem. Biophys. 357*, 111–120.

(46) Veech, R. L., Eggleston, L. V., and Krebs, H. A. (1969) The redox state of free nicotinamide-adenine dinucleotide phosphate in the cytoplasm of rat liver. *Biochem. J. 115*, 609–619.

(47) Penning, T. M., Burczynski, M. E., Jez, J. M., Hung, C. F., Lin, H. K., Ma, H., Moore, M., Palackal, N., and Ratnam, K. (2000) Human 3α-hydroxysteroid dehydrogenase isoforms (AKR1C1-AKR1C4) of the aldo-keto reductase superfamily: functional plasticity and tissue distribution reveals roles in the inactivation and formation of male and female sex hormones. *Biochem. J. 351*, 67–77.

(48) Penning, T. M., and Drury, J. E. (2007) Human aldo-keto reductases: Function, gene regulation, and single nucleotide polymorphisms. *Arch. Biochem. Biophys. 464*, 241–250.

(49) Delescluse, C., Ledirac, N., de Sousa, G., Pralavorio, M., Botta-Fridlund, D., Letreut, Y., and Rahmani, R. (1997) Comparative study of CYP1A1 induction by 3-methylcholanthrene in various human hepatic and epidermal cell types. *Toxicol. in Vitro 11*, 443–447.

(50) Shimada, T., Gillam, E. M., Oda, Y., Tsumura, F., Sutter, T. R., Guengerich, F. P., and Inoue, K. (1999) Metabolism of benzo[*a*]pyrene to *trans*-7,8-dihydroxy-7,8-dihydrobenzo[*a*]pyrene by recombinant human cytochrome P450 1B1 and purified liver epoxide hydrolase. *Chem. Res. Toxicol. 12*, 623–629.

(51) Schwarz, D., Kisselev, P., Cascorbi, I., Schunck, W. H., and Roots, I. (2001) Differential metabolism of benzo[*a*]pyrene and benzo[*a*]pyrene-7,8-dihydrodiol by human CYP1A1 variants. *Carcinogenesis 22*, 453–459.

(52) Shimada, T., Oda, Y., Gillam, E. M., Guengerich, F. P., and Inoue, K. (2001) Metabolic activation of polycyclic aromatic hydrocarbons and other procarcinogens by cytochromes P450 1A1 and P450 1B1 allelic variants and other human cytochromes P450 in *Salmonella typhimurium* NM2009. *Drug Metab. Dispos. 29*, 1176–1182.

(53) Kisselev, P., Schwarz, D., Platt, K. L., Schunck, W. H., and Roots, I. (2002) Epoxidation of benzo[*a*]pyrene-7,8-dihydrodiol by human CYP1A1 in reconstituted membranes. Effects of charge and nonbilayer phase propensity of the membrane. *Eur. J. Biochem. 269*, 1799–1805.

(54) Mammen, J. S., Pittman, G. S., Li, Y., Abou-Zahr, F., Bejjani, B. A., Bell, D. A., Strickland, P. T., and Sutter, T. R. (2003) Single amino acid mutations, but not common polymorphisms, decrease the activity of CYP1B1 against (-)benzo[*a*]pyrene-7R-*trans*-7,8-dihydrodiol. *Carcinogenesis 24*, 1247–1255.

(55) Ratnam, K., Ma, H., and Penning, T. M. (1999) The arginine 276 anchor for NADP(H) dictates fluorescence kinetic transients in 3α-hydroxysteroid dehydrogenase, a representative aldo-keto reductase. *Biochemistry 38*, 7856–7864.

(56) Reiss, P. D., Zuurendonk, P. F., and Veech, R. L. (1984) Measurement of tissue purine, pyrimidine, and other nucleotides by radial compression high-performance liquid chromatography. *Anal. Biochem. 140*, 162–171.

(57) Stocchi, V., Cucchiarini, L., Magnani, M., Chiarantini, L., Palma, P., and Crescentini, G. (1985) Simultaneous extraction and reverse-phase high-performance liquid chromatographic determination of adenine and pyridine nucleotides in human red blood cells. *Anal. Biochem. 146*, 118–124.

(58) Stocchi, V., Cucchiarini, L., Canestrari, F., Piacentini, M. P., and Fornaini, G. (1987) A very fast ion-pair reversed-phase HPLC method for the separation of the most significant nucleotides and their degradation products in human red blood cells. *Anal. Biochem. 167*, 181–190.

(59) Erlemann, K. R., Cossette, C., Grant, G. E., Lee, G. J., Patel, P., Rokach, J., and Powell, W. S. (2007) Regulation of 5-hydroxyeicosanoid dehydrogenase activity in monocytic cells. *Biochem. J. 403*, 157–165.

(60) Spivack, S. D., Hurteau, G. J., Fasco, M. J., and Kaminsky, L. S. (2003) Phase I and II carcinogen metabolism gene expression in human lung tissue and tumors. *Clin. Cancer Res. 9*, 6002–6011.

(61) Shervington, A., Mohammed, K., Patel, R., and Lea, R. (2007) Identification of a novel co-transcription of P450/1A1 with telomerase in A549. *Gene 388*, 110–116.

(62) Ramet, M., Castren, K., Jarvinen, K., Pekkala, K., Turpeenniemi-Hujanen, T., Soini, Y., Paakko, P., and Vahakangas, K. (1995) p^{53}Protein expression is correlated with benzo[*a*]pyrene-DNA adducts in carcinoma cell lines. *Carcinogenesis 16*, 2117–2124.

(63) Jiang, H., Gelhaus, S. L., Mangal, D., Harvey, R. G., Blair, I. A., and Penning, T. M. (2007) Metabolism of benzo[*a*]pyrene in human bronchoalveolar H358 cells using liquid chromatography-mass spectrometry. *Chem. Res. Toxicol. 20*, 1331–1341.

(64) Dohr, O., and Abel, J. (1997) Transforming growth factor-β_1 coregulates mRNA expression of aryl hydrocarbon receptor and cell-cycle-regulating genes in human cancer cell lines. *Biochem. Biophys. Res. Commun. 241*, 86–91.

(65) O'Connor, T., Ireland, L. S., Harrison, D. J., and Hayes, J. D. (1999) Major differences exist in the function and tissue-specific expression of human aflatoxin B_1 aldehyde reductase and the principal human aldo-keto reductase AKR1 family members. *Biochem. J. 343*, 487–504.

(66) Burczynski, M. E., Lin, H. K., and Penning, T. M. (1999) Isoform-specific induction of a human aldo-keto reductase by polycyclic aromatic hydrocarbons (PAHs), electrophiles, and oxidative stress: implications for the alternative pathway of PAH activation catalyzed by human dihydrodiol dehydrogenase. *Cancer Res. 59*, 607–614.

(67) Wang, X. J., Hayes, J. D., and Wolf, C. R. (2006) Generation of a stable antioxidant response element-driven reporter gene cell line and its use to show redox-dependent activation of Nrf2 by cancer chemotherapeutic agents. *Cancer Res. 66*, 10983–10994.

(68) Gates, K. S. Abstracts, American Chemical Society Division of Chemical Toxicology, 234th ACS National Meeting, Boston, MA, August 19–23, 2007, *Chem. Res. Toxicol.* 2007, *20*, 1989−2019; Abstract 139, Penning, T. M.; Park, J. H.; Tacka, K. A.; Quinn, A. M.; Mangal, D.; Blair, I. A. Aldo-keto reductases (AKR) and the metabolic activation of *trans*-7,8-dihydroxy-7,8-dihydrobenzo[*a*]pyrene (B[*a*]P-7,8-dihydrodiol) in human lung adenocarcinoma (A549) cells. p 2017.

TX700345V